Structure and resistance to mechanical stress and enzymatic cleaning of Pseudomonas fluorescens biofilms formed in fresh-cut ready to eat washing tanks

Charles Cunault, Christine Faille, Almudena Calabozo-Delgado, Thierry Benezech

Structure and resistance to mechanical stress and enzymatic cleaning of *Pseudomonas fluorescens* biofilms formed in fresh-cut ready to eat washing tanks.

Author and contact details:

Charles Cunault[b], Christine Faille[a], Calabozo-Delgado Almudena [c], Thierry Benezech[a*]

[a]UMR UMET, INRA, CNRS, Univ. Lille, 59650, Villeneuve d'Ascq, France

[b]UMR1208 IATE, Université de Montpellier, 34095, Montpellier, France

[c] Realco, 15 Avenue Albert Einstein, 1348 Louvain-la neuve, Belgique

*Corresponding author: Thierry Bénézech

***Keywords*:**

Biofilm structure, mechanical detachment, enzymatic cleaning, equipment design, *Pseudomonas fluorescens*, wetting front

Highlights:

- Biofilm formation and structure are strongly related to the equipment design
- Resistant biofilms are observed on surfaces at the wetting front
- Biofilms grown under mechanical stress are highly resistant to shear stress
- Biofilms grown on horizontal surfaces are difficult to clean by enzymes

1. Introduction

Biofilms are of concern in the food industry, in particular in food processing lines having a negative impact on food quality and food safety and subsequent economic losses (Kusumaningrum et al., 2003). Indeed, much has been written on problems caused by both pathogens and food spoilage bacteria within biofilms (Chmielewski and Frank, 2003). Issues have been reported in various food industries e.g. dairy, poultry, meat fish processing industries (Srey et al., 2013). Among the numerous parameters affecting biofilm formation, the equipment design, including material topography and physico-chemistry would appear to play a major role (Faille et al., 2018). Indeed, biofilms are often found in specific areas including those with surface irregularities (e.g. the rough surface of gaskets or welds or grain boundaries of stainless steel surfaces) and those affecting flow patterns (e.g. dead ends, corners). When biofilms were formed under dynamic conditions, their 3D structures were deeply affected by the flow pattern (Manz et al., 2005; Simões et al., 2006; Stoodley et al., 1999b). More compact and less porous biofilms were observed under turbulent flows than under laminar flow conditions (Stoodley et al., 1999a; Vieira et al., 1993). It has been also stated that biofilm formed under dynamic conditions are healthier and more biologically active than those formed in static conditions (Rochex et al., 2008).

Whatever their formation process once established, biofilms are extremely difficult to control through maintenance procedures, since they are both highly resistant to detachment during cleaning procedures (Bénézech and Faille, 2018; Lemos et al., 2015), as well as being strongly resistant to inactivation during disinfection. In addition, turbulent conditions during biofilm formation would result in biofilms which are more resistant to chemical and mechanical stresses (Chmielewski and Frank, 2003; Lemos et al., 2015; Simões et al., 2006).

For over a decade, the presence of interfaces between substratum, liquid and air has been also suspected of significantly affecting the installation of biofilms. For example, wetting front surfaces would be favourable to bacterial adhesion, as well as to the formation and/or the persistence of biofilms (Giaouris and Nychas, 2006; Wijman et al., 2007; Li et al., 2015). As a consequence, equipment whether partly filled during a process, or where residual liquid has remained after a production cycle, provide ready sites for biofilm formation (Wijman et al., 2007; Cunault et al., 2015) and would therefore contribute to the recurrent contamination of food during further production cycles.

Many efforts have been made to control biofilm development by preventive and curative approaches (Srey et al., 2013). Several strategies have been developed in attempts to prevent biofilm installation, primarily by acting on surface material properties, equipment design, as well as process

conditions including flow patterns. Removal strategies *i.*e. the development of efficient cleaning and disinfection procedures have focused mainly on chemical compounds (cleaning and biocide agents) and application means (contact time, temperature).

The aim of this study was to investigate the role of flow patterns and equipment design features, on the biofilm structure after one, two or three days and on their further resistance to chemical vs mechanical actions occurring potentially during cleaning procedures. For this purpose, a series of mock-ups of industrial washing tanks for the fresh-cut food industry (Cunault et al., 2018) was used to study the contamination schemes of *Pseudomonas fluorescens* biofilms. Resistance to mechanical action was analysed using a flow cell under microscope (Faille et al., 2016) and resistance to cleaning was studied using enzymes in line with industrial foam cleaning practices.

2. Material and method

2.1. Biological material

P. fluorescens PF1, isolated by ANSES from waste cleaning water, was selected as a model of spoilage bacteria for fresh food industry due to its ability to grow and form biofilms at 10 °C (Charles Cunault et al., 2015).

2.2. Pilot rig

Experiments were performed on a pilot rig (Figure 1) specially designed to mimic the various conditions found in the industrial washing tanks typically employed for fresh cut food products (Cunault et al., 2015). This device is composed of three parts: 1/ the square tube section wherein the flow is unidirectional and turbulent, 2/ the entry vat wherein quasi static conditions are found and 3/ a series of test vats filed by cascade flow providing 3D flow conditions, where fluid is agitated by a Rushton impeller. The device was filled with 73.5 L of liquid maintained at 10°C and was set at a flow rate of 150 $L.h^{-1}$. According to (Cunault et al., 2015) such flow conditions induce a mean wall shear stresses of 0.45 Pa in the square tubes. In the test vats, the mean wall shear stresses depended on the coupon's location: 0.1 Pa at the corners, between 0.1 and 0.5 Pa in the folded and welded areas, between 0.25 and 4 Pa at the horizontal and vertical flat surfaces.

Stainless steel slides of AISI 316 with a 2B finish were placed in the different sections of the rig to follow the formation or detachment of biofilms. Flat slides (1.5 x 4.5 mm^2) were inserted in the square tubes or placed against the inside surfaces of vats. Right-angled coupons, obtained by folding

98 or welding, were also placed on the vat surface.

99

100 *2.3. Biofilm formation*

101

102 Biofilms were grown in the rig at 10°C in TSB diluted 1/10 (Tryptone Soy Broth, Biokar, Beauvais,
103 France) inoculated at 10^6 CFU.mL^{-1} with an overnight culture of *P. fluorescens* (TSB, 30 °C). Biofilms
104 were formed during 24, 48 and 72 h. The surface microbial load, the biofilm structure (SEM
105 observation), and resistance to foam cleaning and mechanical detachment were investigated after
106 24, 48, and 72 h after rinsing in reverse osmosed water. Details are given in Table 1.

107

108 *2.4. Biofilm analysis*

109

110 In order to estimate the amount of biofilms in terms of CFU, biofilms were sampled using cotton
111 swabs (Copan, Brescia, Italy) from the surface of coupons in contact with the suspension. The swabs
112 were previously soaked with peptone water diluted 1/10 with 0.5% V/V Tween 80 (Sigma-Aldrich,
113 France). Two swabs were used per sample and put into a single container with 10 mL of the peptone-
114 Tween solution. They were subjected to an ultrasonication step (2.5 min, Ultrasonic bath, Deltasonic,
115 France) in order to release bacteria from the swab and to homogenize the suspension. The detached
116 bacteria were enumerated on TSA (Tryptone Soy Agar, Biokar, France) after 48 h at 30°C.
117 The biofilm structure was observed by scanning electron microscopy (SEM). As biofilms were
118 easily removed from the surfaces, the contaminated slides were carefully rinsed in osmosed water at
119 a low flow rate for 3 min. The biofilms were then fixed in a 1.25% glutaraldehyde, 0.1 mM sodium
120 cacodylate (pH7) buffer for 48 h, then immersed overnight in a 2% osmium tetraoxide solution,
121 dehydrated in an ethanol series and lastly subjected to critical point drying. Dehydrated biofilms
122 were then coated with gold-palladium for 1.5 min and viewed on an S-3000 Hitachi scanning electron
123 microscope operating at 20 kV.

124

125 *2.5. Biofilm resistance to cleaning*

126

127 Biofilm resistance to cleaning was performed using an enzyme foaming agent provided by Realco®
128 (Realco, Louvain-la-Neuve, Belgium). The foam was composed of 0.2% Biorem 20 (enzymatic mix)
129 and 1% Enzyfoam (surfactant and enzymes). The enzymatic mix included proteases and
130 polysaccharidases previously shown to efficiently remove biofilms (Lequette et al., 2010). Prior to
131 use, the cleaning solution was placed at 45°C for 30 min to activate the enzymes. The foam was
132 diluted to 5% in the foam gun and applied twice for 10 min of contact time each. Prior to

133 enumeration, surfaces were rinsed twice by streaming of osmosed water and then dried for 30 min
134 at 30 °C. The number of residual cultivable cells was estimated as described in Section 2.3, and the
135 biofilm detachment was assessed by comparing the numbers of adherent bacteria before and after
136 cleaning. Any potential effect on the bacteria viability of the chosen enzymatic detergent (mixture of
137 enzymes and surfactant) was checked. Biofilms were therefore covered with the foam for 10 min and
138 the number of cultivable cells within these treated biofilms was compared to those of untreated
139 biofilms. The variance analysis (p=0.71) indicated that the treatment had no significant effect on the
140 number of cultivable cells (data not shown).
141
142 *2.6. Biofilm resistance to mechanical detachment (water flow)*
143
144 In order to monitor biofilm resistance to detachment, a parallel-plate flow chamber with a
145 rectangular flow channel (60-mm length by 5-mm width and 0.5-mm height) designed at INRA-PIHM
146 (Faille et al., 2016) was used. For this purpose, contaminated coupons stained with 0.01% Acridine
147 Orange (Sigma-Aldrich) were put into the flow chamber and subjected to 30-second steps of
148 increasing flow rates of deionised water at room temperature (wall shear stresses of 17, 33, 93, 167,
149 241, and 310 Pa).
150 The bacterial detachment over time was monitored under microscope (Axioskop 2 plus, Zeiss) by
151 epifluorescence on an area of about 130 × 100 µm², which is considered to be representative of the
152 whole surface contamination. Images at T0 and at the end of each detachment step were recorded
153 by camera (Olympus DP21, France) at a magnification of x400. The number of adherent cells or,
154 when the coverage was too high for cell enumeration, the percentage of surface covered with
155 biofilms were quantified using image analysis (ImageJ software). Biofilm detachment was assessed by
156 the ratio of the number of cells remaining after each flow rate step to the number of cells at T0.
157
158 *2.7. Statistical analyses*
159
160 Two sets of experiments were conducted. For each set of experiments, trials were carried out at least
161 in triplicate, with at least two coupons for each trial.
162 Data were analysed by general linear model procedures using SAS V9.4 software (SAS Institute, Gary,
163 NC, USA). Variance analyses were performed to determine the impact of coupon location, age of
164 biofilm and trial, on the amount of biofilm in terms of CFU. These were followed by multiple
165 comparison procedures using Tukey's grouping (Alpha level = 0.05). Other sets of variance analyses
166 and Tukey's grouping were performed to determine: the role of coupon location, the age of the
167 biofilm, the trial, the wall shear stress or enzyme action on the biofilm detachment.

168

169 **3. Results**

170

171 *3.1. Biofilm formation*

172

173 The average numbers of cultivable cells on each area (square tubes, entry vat (H-static and V-
174 static) and reference vats (other areas) are given in Table 2. After 24 h growth, clear differences were
175 observed in the numbers of cultivable cells (between 7.8 and 1.3 10^6 CFU.cm^{-2}). The vertical (V-VAT)
176 flat surface of the test vats was the least contaminated. Four other areas were poorly contaminated
177 with between 1.2 10^3 and 7.4 10^3 CFU.cm^{-2}, namely the other two flat surfaces, horizontal (H-VAT)
178 and partially immersed surfaces corresponding to a wetting front (Interface), but also the vertical
179 weld (V-WELD) and horizontal fold (H-FOLD). Lastly, the greatest amounts of biofilm were observed
180 on both horizontal (H-STAT) and vertical (V-STAT) surfaces in the entry vat (quasi-static conditions).
181 Whatever the area, the surface contamination further increased with time to reach values ranging
182 from 3.1 10^5 to 1.9 10^8 CFU.cm^{-2} after 72 h. The V-VAT were still poorly contaminated, followed by
183 the H-FOLD, but the observed differences were less pronounced than after 24 h. It is noteworthy that
184 both surfaces of the entry vat (H- and V-STA), in quasi-static conditions, were still among the three
185 most contaminated surfaces, whatever the duration of biofilm formation. The newly highly
186 contaminated coupons were those inserted into the tubes.

187 Statistical analysis confirmed these observations. The variance analysis, which took into account
188 the biofilm location, trial and duration of biofilm formation (Table 3), showed that the three
189 parameters accounted for 76% of the variability and that each played a significant role ($p<0.0001$).
190 Further variance analyses were performed for each duration of biofilm formation. The differences
191 observed in the number of CFU on the different areas were still largely attributed to the two
192 remaining parameters (location and trial type), at least at 24 h (83% of the variability) and at 48 h
193 (74%). Results also clearly indicated that the amount of CFU was affected by the biofilm location ($p <$
194 0.0001). The influence of the trial increased with the age of the biofilm, to become significant after
195 72 h.

196 According to the Tukey's groupings performed for each duration of biofilm formation (Table 2),
197 significant differences were observed between some locations. For example, the H- and V-STATIC
198 locations (quasi-static conditions) were significantly more contaminated than the surfaces of the test
199 Vats, except the corners (at 24, 48 and 72 h) and the H-WELD (at 24 h). On the other hand, the
200 vertical surfaces of the vats (V-VAT) were significantly the least contaminated whatever the biofilm
201 age. However, biofilms grown at the interface being also on a vertical wall appeared to be at an
202 intermediate level. On the other hand, the vertical surfaces of the vats (V-VAT) were significantly the

203 least contaminated surface, whatever the of biofilm age. However, biofilms grown at the interface
204 being also on a vertical wall were at an intermediate contamination level.
205
206 *3.2. The SEM observations*
207
208 SEM observations were performed on 72 h-biofilms produced on coupons inserted into square
209 tubes or placed against the surfaces of the entry and test vats. Due to difficulties encountered in
210 maintaining coupons in position in the H-VAT and V-VAT, the observation of vertical and horizontal
211 surfaces of the test-vats was performed on the horizontal and vertical sides of the H-WELD and H-
212 FOLD coupons.
213 The amount and distribution of biofilms over the tested surfaces are shown in Figures 2 and
214 supplementary data 1. The distribution largely depended on the sampling zone. For example, the
215 highest bacterial density was observed at the interface zone (Figure 2, left part), while surfaces
216 located at the welds or the folds (Supplementary File 1) were only slightly contaminated with the
217 presence of few clusters (mainly located in the surface defects) separated by wide zones with single
218 cells or devoid of any contamination. These results are broadly consistent with the enumeration
219 data. Concerning the biofilm structures (Figures 2 and 3), cell clusters or even 3-D structures were
220 clearly observed on most surfaces, suggesting the presence of complex biofilms along with single
221 cells or small cell clusters. As visible on the surface of the square tube, cell clusters were sometimes
222 long and narrow, forming ripple-like structures mainly parallel to the flow direction (white arrow).
223 Small ridge-like structures were also seen on the H-WELD and H-FOLD surfaces, but their orientation
224 was strongly affected by their location (vertical side, horizontal side, bending/welding areas)
225 probably as the result of flow organisation. Conversely, those clusters formed in static conditions
226 were rounded (V- and H-STAT) or slightly elongated in all directions (H-STAT). Lastly at the interface
227 (Figure 3), the dense cell clusters were flat and interspersed with poorly contaminated areas in the
228 fully immersed zone, seeming to coalesce to form large and flat aggregates in the intermittently
229 immersed interface zone.
230 In order to observe the biofilm structures in detail, further observations were performed at
231 stronger magnification (Figures 3-A, -B and –C and Supplementary data 1). Extracellular material was
232 clearly observed when biofilms were produced in tubes (Supplementary data 1-A, white arrow),
233 while at best, only small quantities of exopolymers were produced in the other areas (Supplementary
234 data 1-B, -D and -H). Anecdotally, it can also be noted that many bacteria were located in the depth
235 of grain boundaries on the upper part of the interface zone (Figure 3-A) and that these surface
236 irregularities would probably provide protection against shear stresses during process and during
237 hygiene procedures.

238

239 *3.3. Mechanical resistance*

240

241 Five areas (flat surfaces) were kept for further experiments on bacterial detachment in the flow
242 cell under microscope. Detachment experiments were performed at increasing wall shear stresses
243 (17, 60, 130, 190, 275, and 360 Pa) using deionised water at room temperature. As shown in Figure 4,
244 great differences in the resistance to detachment were obtained regardless of the age of the biofilms
245 (Figures 4-A, -B and -C): biofilms grown on V-VAT and at interface were systematically the most
246 resistant to detachment. Elsewhere, most biofilms became more resistant to detachment with time,
247 such as biofilms at interfaces, whose percentage of residual biofilm increased from 74% after 24 h to
248 90% after 48 h of biofilm growth. The contrary was observed when biofilms were grown in V-VAT
249 conditions with average values of 87, 83 and 72% residual biofilm after 24 h, 48 h, and 72 h,
250 respectively. Concerning the influence of shear stress, little (<20%) or no detachment was observed
251 at 17 Pa. Conversely when biofilms were subjected to higher shear stresses, great differences were
252 observed between areas in the ease of biofilm detachment, with percentages of residual biofilm
253 ranging from less than 10% (24 h-biofilms in V-STAT, H-STAT and pipes) to around over 75% (48 h-
254 and 72 h-biofilms at the interface).

255 Taking into account the whole set of data (Table 4), the variance analysis indicated that all the
256 three parameters: wall shear stress (WSS), location, and trial type significantly affected the resistance
257 of biofilms to detachment (p-values < 0.0001, <0.0001, =0.0005, respectively), while the age of
258 biofilms did not (p=0.1162). Further variance analyses were performed for each wall shear stress. As
259 shown in Table 4, the ease of removal of biofilms was significantly affected by the biofilm location,
260 whatever the shear stress (p<0.0001), yet not at all or only to a very limited extent by the age of
261 biofilms. Tukey's grouping showed that, regardless of the wall shear stress, the amount of residual
262 biofilm was one of the highest when biofilm growth occurred at the interface and one of the lowest
263 when biofilm growth occurred in H-STAT conditions.

264

265 *3.4. Resistance to enzymatic cleaning*

266

267 Data are presented in Figure 5. Great differences among zones were observed in the residual ratio
268 of biofilms after cleaning varying from 1 (no removal) down to 0.01 (99% removal). The most difficult
269 to clean areas to clean were the three horizontal surfaces and the corner. A wide distribution of the
270 data could be observed in these areas. Conversely, vertical areas and coupons located in tubes were
271 more cleanable with a lower range of data distribution. Interface area data differed from the other
272 cases by a wide variability comparable to those areas difficult to clean and by a low median value

273 comparable to easy-to-clean areas. SEM observations of H-FOLD and H-WELD in Supplementary File 2
274 confirmed the low cleanability of both locations with a significant remaining amount of bacteria, but
275 without any visible clusters. Conversely, SEM observations showed that a significant residual
276 contamination was also present on the surfaces located at the interface, with the presence of cell
277 clusters.

278 The analysis of variance (Table 4) indicated that the location and trial type significantly affected
279 the resistance of biofilms to detachment (p-values < 0.0001, =0.0122 respectively), while the age of
280 biofilms did not (p=0.91). Tukey's grouping (Table 5.2) confirmed that biofilms grown on horizontal
281 surfaces comprising design defaults (welds, folds and corners (group A)) were more difficult to clean
282 than vertical surfaces and tubes (group C). Lastly, the interface residual ratio was at an intermediate
283 level (group ABC), due to the wide variation between trials.

284

285 **4. Discussion**

286 Experiments were carried out with mock-ups of vats designed to be close to those encountered in
287 the fresh-cut food industry including pipes commonly present in processing lines. The vat design was
288 chosen to reproduce some specific features to evidence their criticality in terms of hygiene while
289 circulating water contaminated with a *Pseudomonas* strain. A strong influence of the design on
290 biofilm development and shape and their further resistance to shear stress and enzymatic cleaning
291 was clearly observed. Available literature reports numerous studies on how the flow conditions
292 affect biofilm formation and properties. Some authors (Chmielewski and Frank, 2003; Dunsmore et
293 al., 2002; Purevdorj et al., 2002; Stoodley et al., 1999b) and more recently (Brugnoni et al., 2011,
294 2012); Hödl et al., 2014) have shown that unidirectional flow reduces the degrees of freedom of
295 migrating cells and cluster coalescence to spread spatially, thereby inducing elongated shape biofilm
296 structures. This phenomenon induces the cluster anisotropy clearly observed in this study for
297 biofilms grown in pipes. However, such elongated shape clusters were also observed for biofilms
298 formed in vats in every area largely affected by the flow recirculation induced by the impeller, either
299 on bend zones (with welds or not), or simply on vertical and horizontal surfaces. Such a pattern is
300 different from the ripple-shaped pattern (perpendicular to the flow) described by (Cogan et al.,
301 2018), taking into account the oscillatory phenomenon induced by the flow. In addition to the
302 morphology, hydrodynamics affects cell density and biofilm matrix composition. The fluid velocity
303 field in contact with the attached microbial layer is widely considered as one of the most important
304 factors affecting biofilm structure and activity (Araújo et al., 2016; Liu and Tay, 2002; Pereira et al.,
305 2002) greatly exceeding the influence of factors such as biofilm age, suspended cell concentration,
306 pH, surface roughness of the substratum (Chen et al., 2005). Indeed, biofilm volumetric density and
307 EPS volume increase with the shear stress, resulting in an increased biofilm cohesion (Garny et al.,

308 2008; Simões et al., 2010). Such statements were confirmed here with a stronger resistance to shear
309 of observed for biofilms grown under dynamic conditions on the vat walls directly affected by the
310 flow movements induced by the impeller. Hence, such biofilms were the ones presenting the most
311 remarkable increased between 24h and 72h with almost 5 Log. Santos et al. (1991) reported much
312 thicker biofilms of *P. fluorescens* at 2.5 m s^{-1} than at 0.5 m s^{-1} leading to a more stable biofilm. In
313 addition, V-Vat biofilms presented oriented clusters due probably to the flow arrangement at the
314 wall surface as previously observed (Brugnoni et al., 2012). Cells in contact with flowing become
315 oriented so that each cell offers the least resistance to flow possibly corresponding to the natural
316 elimination of cells susceptible to shear forces when the biofilm grow due to their position in relation
317 to the flow. It should be mentioned that very high shear stresses (over 300 Pa) were used here,
318 while those encountered in food processing lines barely exceed 100 Pa. Such a high resistance to the
319 shear stress was also observed for biofilm grown at the interface. This resistance could be the result
320 of the conditions encountered during biofilm formation at the wetting front along with the periodic
321 wetting induced by the impeller rotation. Even if it is not at the same scale wetting front detrimental
322 effects are known in other environment as marine environment but not in terms of biofouling but in
323 terms of active corrosion. All splash areas were found to deeply limit the lifespan of reinforced
324 concrete marine structures and considered as accelerated high water corrosion zone compared to
325 low water corrosion zones that pass from air, i.e. above high tide level into sea water to below low
326 tide level (Mackie, 2008). However, it is largely admitted that thick biofilms often preferentially
327 develop at the interface, rather than in wholly submerged areas. Biofilms at the interface has been
328 reported in the literature, but only in laboratory conditions. Some authors including (Wijman et al.,
329 2007) have suggested that such biofilms may develop particularly in partly-filled devices such as
330 industrial storage and piping systems during process or after the cleaning procedure in areas with
331 residual liquid. All these surfaces should be recognized as actual critical points in terms of surface
332 hygiene in the food processing lines or environments.

333 A recent review (Nahar et al., 2018) described the advances in biofilm impairment strategies in
334 the food industry. Among these strategies, enzymes were put forward as an alternative to chemical
335 agents as previously demonstrated (Lequette et al., 2010). Commercial enzyme formulations contain
336 mixtures of enzymes with different substrate spectra. Enzymatic processes have the advantage of
337 disaggregating biofilm clumps rather than just removing them from the surface, as is the case with
338 mechanical action (Bridier et al., 2011). According to a recent work performed in our laboratory on
339 Cleaning-In-Place kinetics of surfaces contaminated by *Pseudomonas fluorescens* biofilms (Bénézech
340 and Faille, 2018), the NaOH chemical action acted mainly on the biofilm matrix, inducing a disruption
341 of the clusters at the early phase of the kinetics, while the mechanical action also acted on the cells
342 directly in contact with the surface. When using an enzymatic cocktail, the ease of cleaning was

enhanced for vertical surfaces compared to horizontal ones, interface biofilms being at an intermediate level. Biofilms in tubes also appeared to be less resistant to enzymes. Conversely, the dynamic vs static conditions during biofilm growth did not affect the cleaning efficiency. (Lemos et al., 2015) working on *Bacillus* biofilms, did not find any influence on the cleaning efficiency of the growth conditions, turbulent or laminar either. In this work, despite their specific surface features, welds surprisingly were cleanable when vertical but not when horizontal. This is in line with previous papers stating no relationship between welding zones and bacterial adhesion (Casarin et al., 2014) or bacterial colonization (Tide et al., 1999). Nevertheless, the resistance to cleaning seems to be related to the design features in accordance to EHEDG principles (Hofmann et al., 2018), which states that horizontal surfaces and corners should be avoided. Lastly the interface zone which can be considered to be hygienic according to EHEDG (vertical wall) appeared here to be poorly hygienic. Any surface regularly splashed without regular cleaning and prone to drying, may therefore represent hygienic issues, which are likely to result in a resident contamination in the factory site. Design requirements stated in the sole European standard concerning the basic concepts on hygiene requirements of food processing machineries (EN 1672-2:2006+A1:2009 Food processing machinery - Basic concepts - Part 2: Hygiene requirements) differentiates the presence or not of food (food and non-food areas) and the splash area. Splash areas shall be designed and constructed following the same principles for the food areas. The concept of 'no return to the food area' is imperative and lead to less stringent design criteria: in the washing tanks splashed areas are part of the food area as the splashed washing water may contain food (piece of fresh-cut vegetables) being able to go back to the tank to be eventually packed and ready for delivery to the consumer.

5. Conclusion

It was demonstrated in conditions close to those encountered in vegetable processing industry, that some specific areas within industrial washing tanks are prone to allowing a strong bacterial contamination and generating a further high resistance to rinsing/cleaning processes. In addition to those areas already identified as poorly hygienic (welds, corners, horizontal surfaces), the interface zones corresponding to the wetting front should also be considered as a place conducive to the installation of resistant bacterial contamination. Importance of the design appeared here not only in terms of ease of cleaning but in terms of surface contamination. In actual washing tanks in use in the fresh-cut industry, design principals encountered are those of this study washing tanks. Thus, any modifications such as open angles, no horizontal surfaces, no right corners would thus significantly change the contamination scheme and minimise further resistance to cleaning and make the conclusions of this study directly applicable. It should be kept in mind that interface zones should be

considered to improve the hygienic level of the whole equipment and lines. This would allow industrialists to envisage the use of more environmentally-friendly cleaning procedures complying with new environmental constraints.

Acknowledgments

This work was undertaken under the European Research Project SUSCLEAN (contract number FP7-KBBE-2011-5, project number: 28514). We are grateful to Jean-François Migdal, Jacky Six and Laurent Wauquier for their involvement in this work. We also thank the trainees Olivier Behague, Jonathan Braquis and Mickaël Pollet for their valuable contribution.

References:

Araújo, P.A., Malheiro, J., Machado, I., Mergulhão, F., Melo, L., Simões, M. (2016). Influence of Flow Velocity on the Characteristics of *Pseudomonas fluorescens* Biofilms. Journal of Environmental Engineering 142, 04016031.

Bénézech, T., Faille, C. (2018). Two-phase kinetics of biofilm removal during CIP. Respective roles of mechanical and chemical effects on the detachment of single cells vs cell clusters from a *Pseudomonas fluorescens* biofilm. Journal of Food Engineering 219, 121–128.

Bridier, A., Briandet, R., Thomas, V., Dubois-Brissonnet, F. (2011). Resistance of bacterial biofilms to disinfectants: A review. Biofouling 27, 1017–1032.

Brugnoni, L.I., Cubitto, M.A., Lozano, J.E. (2011). Role of shear stress on biofilm formation of *Candida krusei* in a rotating disk system. Journal of Food Engineering 102, 266–271.

Brugnoni, L.I., Cubitto, M.A., Lozano, J.E. (2012). *Candida krusei* development on turbulent flow regimes: Biofilm formation and efficiency of cleaning and disinfection program. Journal of Food Engineering 111, 546–552.

Casarin, L.S., Brandelli, A., de Oliveira Casarin, F., Soave, P.A., Wanke, C.H., Tondo, E.C. (2014). Adhesion of *Salmonella enteritidis* and *Listeria monocytogenes* on stainless steel welds. International Journal of Food Microbiology 191, 103–108.

Chen, M.J., Zhang, Z., Bott, T.R. (2005). Effects of operating conditions on the adhesive strength of Pseudomonas fluorescens biofilms in tubes. Colloids and Surfaces B: Biointerfaces 43(2),61-71

Chmielewski, R.A.N., Frank, J.F. (2003). Biofilm formation and control in food processing facilities. Comprehensive Reviews in Food Science and Food Safety 2, 22-32.

Cogan, N.G., Li, J., Fabbri, S., Stoodley, P. (2018). Computational Investigation of Ripple Dynamics in Biofilms in Flowing Systems. Biophysical Journal 115, 1393–1400.

Cunault, Charles, Faille, C., Bouvier, L., Föste, H., Augustin, W., Scholl, S., Debreyne, P., Benezech, T. (2015). A novel set-up and a CFD approach to study the biofilm dynamics as a function of local flow conditions encountered in fresh-cut food processing equipment. Food and Bioproducts Processing 93, 217–223.

Cunault, C., Faille, C., Briandet, R., Postollec, F., Desriac, N., Benezech, T. (2018). *Pseudomonas sp*. biofilm development on fresh-cut food equipment surfaces – a growth curve – fitting approach to building a comprehensive tool for studying surface contamination dynamics. Food and Bioproducts Processing 107.

Dunsmore, B.C., Jacobsen, A., Hall-Stoodley, L., Bass, C.J., Lappin-Scott, H.M., Stoodley, P. (2002). The influence of fluid shear on the structure and material properties of sulphate-reducing bacterial biofilms. Journal of Industrial Microbiology and Biotechnology 29, 347–353.

Faille, C., Bihi, I., Ronse, A., Ronse, G., Baudoin, M., Zoueshtiagh, F. (2016). Increased resistance to detachment of adherent microspheres and *Bacillus* spores subjected to a drying step. Colloids and Surfaces B: Biointerfaces 143, 293–300.

Faille, C., Cunault, C., Dubois, T., Bénézech, T. (2018). Hygienic design of food processing lines to mitigate the risk of bacterial food contamination with respect to environmental concerns. Innovative Food Science and Emerging Technologies 46, 65–73.

Garny, K., Horn, H., Neu, T.R. (2008). Interaction between biofilm development, structure and detachment in rotating annular reactors. Bioprocess and Biosystems Engineering 31, 619–629.

Giaouris, E.D., Nychas, G.J.E. (2006). The adherence of *Salmonella enteritidis* PT4 to stainless steel: The importance of the air-liquid interface and nutrient availability. Food Microbiology 8, 747-752.

Hödl, I., Mari, L., Bertuzzo, E., Suweis, S., Besemer, K., Rinaldo, A., Battin, T.J. (2014). Biophysical controls on cluster dynamics and architectural differentiation of microbial biofilms in contrasting flow environments. Environmental Microbiology 16(3), 802-812

Hofmann, D.J., Åkesson, S., Curiel, G., Woulters, D.P., Timperley, A. (2018). Hygienic Design Principles. European Hygienic Engineering & Design Group Guidelines 8.

Kusumaningrum, H.D., Riboldi, G., Hazeleger, W.C., Beumer, R.R. (2003). Survival of foodborne pathogens on stainless steel surfaces and cross-contamination to foods. International Journal of Food Microbiology 85, 227 – 236.

Lemos, M., Mergulhão, F., Melo, L., Simões, M. (2015). The effect of shear stress on the formation and removal of *Bacillus cereus* biofilms. Food and Bioproducts Processing 93, 242–248.

Lequette, Y., Boels, G., Clarisse, M., Faille, C. (2010). Using enzymes to remove biofilms of bacterial isolates sampled in the food-industry. Biofouling 26, 421–431.

Li, B., Liu, X.-C., Li, L., Xu, Z.-B. (2015). Molecular identification of the genotype of *Staphylococcus aureus* biofilm. Modern Food Science and Technology 31(7), 74-79.

Liu, Y., Tay, J.H. (2002). The essential role of hydrodynamic shear force in the formation of biofilm and granular sludge. Water Research 36(7),1653-1665.

Mackie, K.P. (2008) Accelerated high water corrosion. in Alexander, M., Beushausen, H.-D., Dehn, F., Moyo, P. (Eds.) (2008). Concrete Repair, Rehabilitation and Retrofitting II: 2nd International Conference on Concrete Repair, Rehabilitation and Retrofitting, ICCRRR-2, 24-26 November 2008, Cape Town, South Africa. CRC Press.

Manz, B., Volke, F., Goll, D., Horn, H. (2005). Investigation of biofilm structure, flow patterns and detachment with magnetic resonance imaging. Water Science and Technology 52, 1–6.

Nahar, S., Mizan, M.F.R., Ha, A.J. won, Ha, S. Do (2018). Advances and Future Prospects of Enzyme-Based Biofilm Prevention Approaches in the Food Industry. Comprehensive Reviews in Food Science and Food Safety 17, 1484–1502.

Pereira, M.O., Kuehn, M., Wuertz, S., Neu, T., Melo, L.F. (2002). Effect of flow regime on the architecture of a *Pseudomonas fluorescens* biofilm. Biotechnology and Bioengineering 78, 164–171.

Purevdorj, B., Costerton, J.W., Stoodley, P. (2002). Influence of hydrodynamics and cell signaling on the structure and behavior of *Pseudomonas aeruginosa* biofilms. Applied and Environmental Microbiology 68(9), 4457-4464.

Rochex, A., Godon, J.J., Bernet, N., Escudié, R. (2008). Role of shear stress on composition, diversity and dynamics of biofilm bacterial communities. Water Research 42(20), 4915-22.

Santos, R., Callow, M.E. and Bott, T.R. (1991) The structure of *Pseudomonas fluorescens* biofilms in contact with flowing systems. Biofouling 4, 319–336.

Simões, M., Simões, L.C., Machado, I., Pereira, M.O., Vieira, M.J. (2006). Control of Flow-Generated Biofilms with Surfactants. Food and Bioproducts Processing 84, 338–345.

Simões, M., Simões, L.C., Vieira, M.J. (2010). A review of current and emergent biofilm control strategies. LWT - Food Science and Technology 43, 573–583.

Srey, S., Jahid, I.K., Ha, S.D. (2013). Biofilm formation in food industries: A food safety concern. Food Control 31, 572–585.

Stoodley, P., Dodds, I., Boyle, J.D., Lappin-Scott, H.M., (1999a). Influence of hydrodynamics and nutrients on biofilm structure. J. Appl. Microbiol. Symposium Supplement 85, 19S-28S.

Stoodley, P., Lewandowski, Z., Boyle, J.D., Lappin-Scott, H.M., (1999b). The formation of migratory ripples in a mixed species bacterial biofilm growing in turbulent flow. Environmental Microbiology 1, 447–455.

Tide, C., Harkin, S.R., Geesey, G.G., Bremer, P.J., Scholz, W. (1999). Influence of welding procedures on bacterial colonization of stainless steel weldments. Journal of Food Engineering 42, 85–96.

Vieira, M.J., Melo, L.F., Pinheiro, M.M. (1993). Biofilm formation: hydrodynamic effects on internal diffusion and structure. Biofouling 7, 67–80.

Wijman, J.G.E., De Leeuw, P.P.L.A., Moezelaar, R., Zwietering, M.H., Abee, T. (2007). Air-liquid interface biofilms of *Bacillus cereus*: Formation, sporulation, and dispersion. Applied and Environmental Microbiology 73(5), 1481–1488.

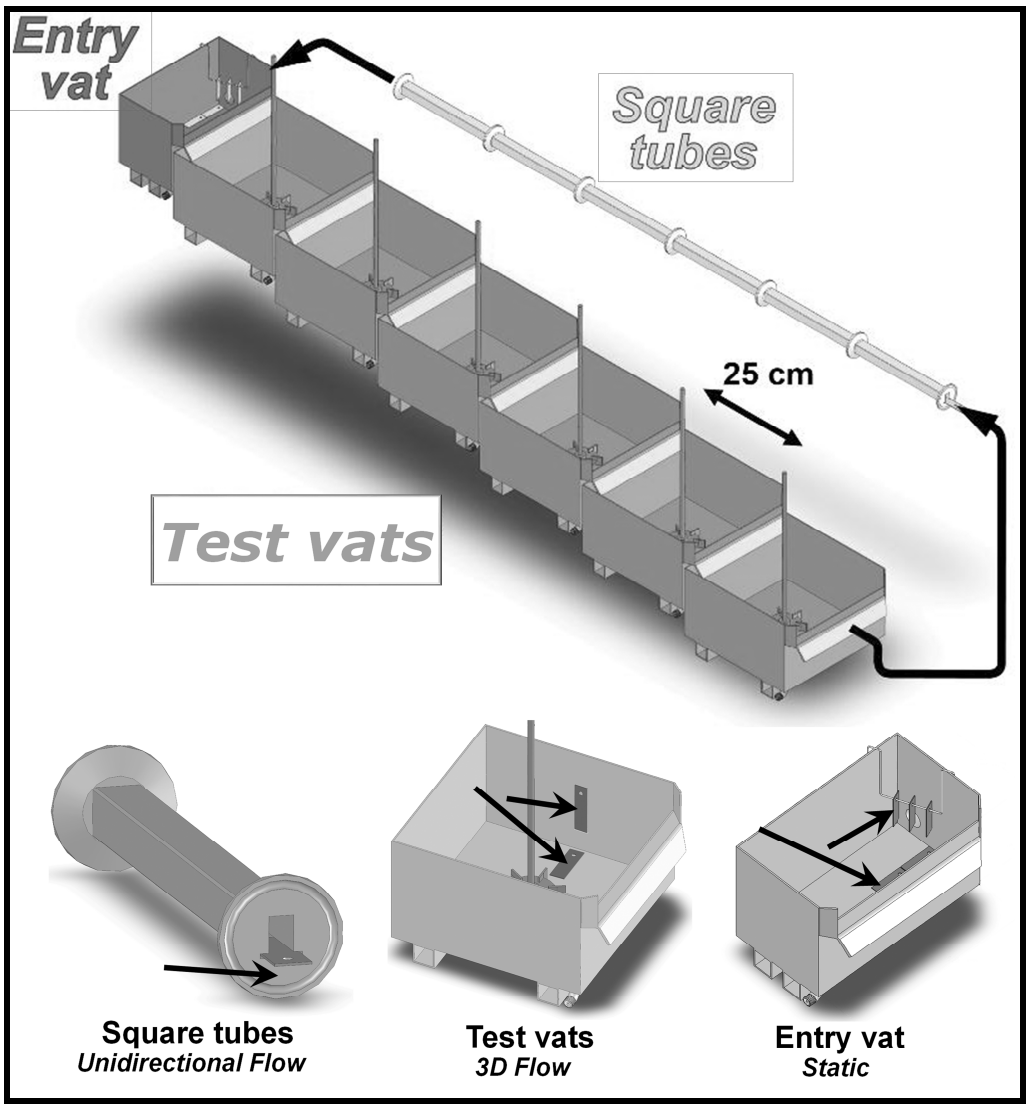

Figure 1: Schematic representation of the pilot rig. The black arrows indicate the location of the coupons.

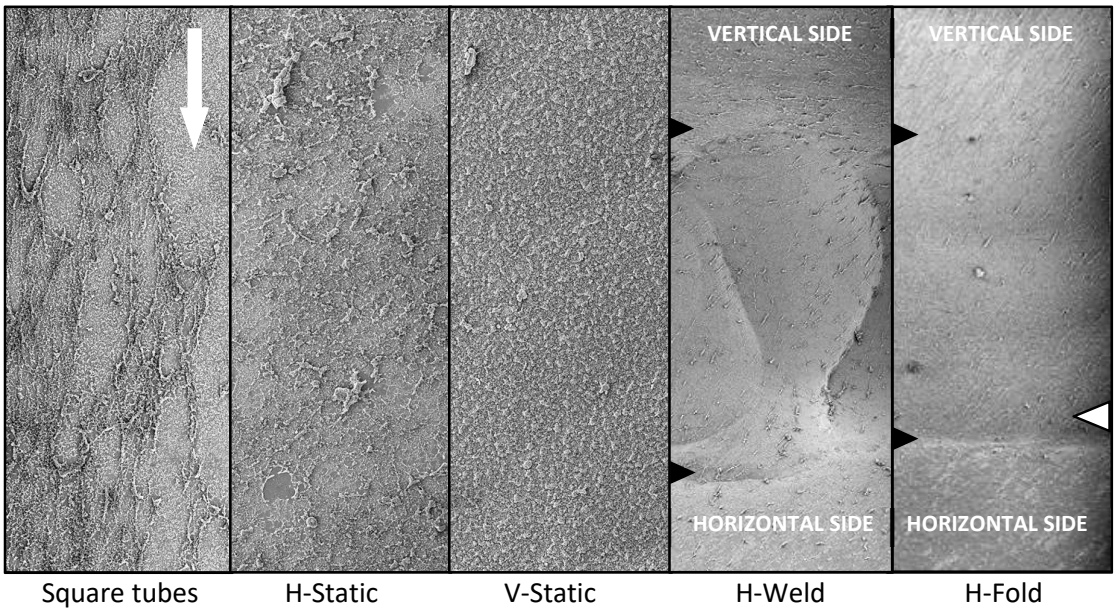

Figure 1: SEM observation of 72 h-biofilms. The white arrows indicate the flow direction. The black triangles indicate the top and bottom threshold between which the angle is located. The white triangle indicates the score line of the folded slides. Magnification x70.

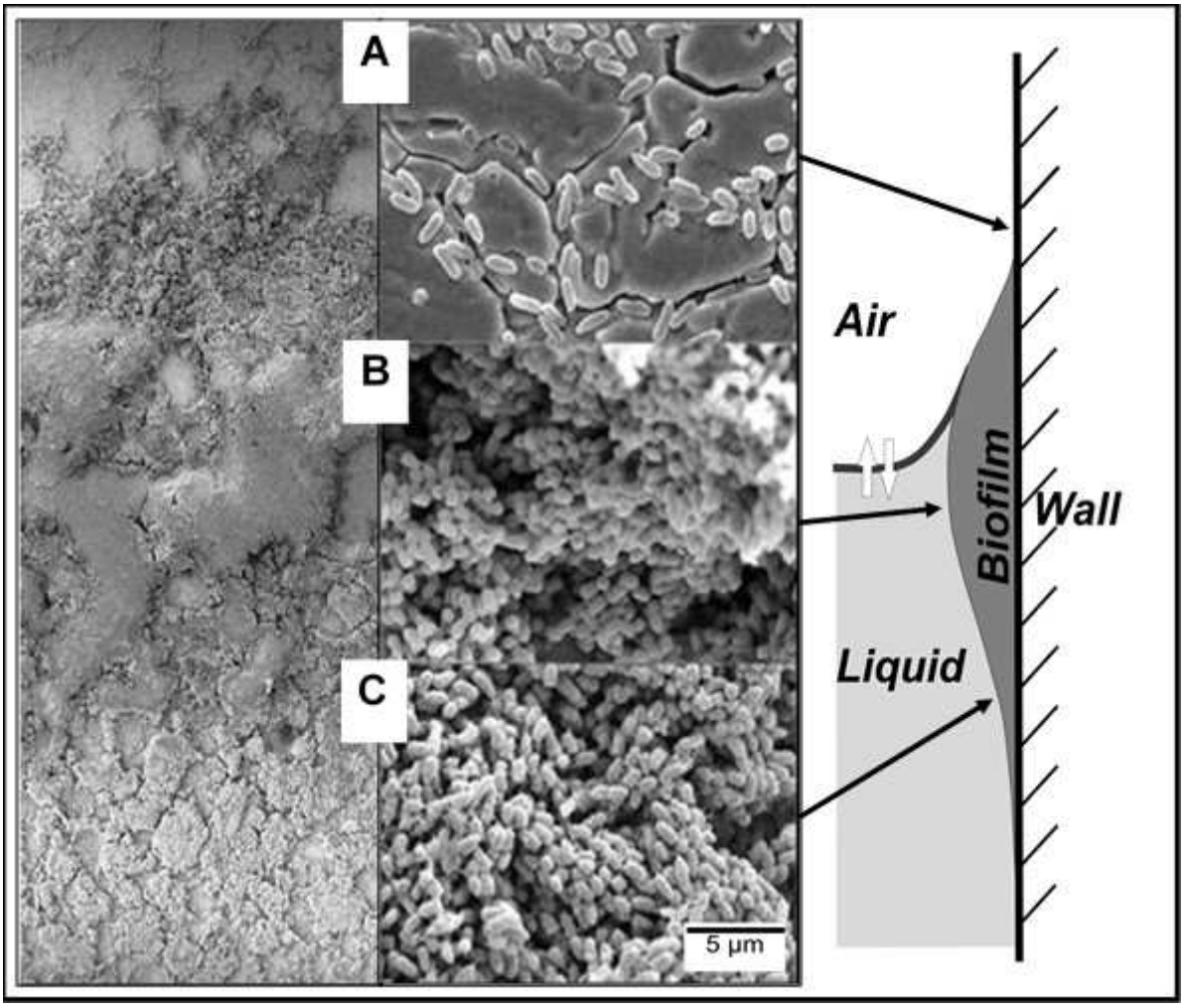

Figure 3: SEM observation of the wetting front (interface). Left part: magnification x70. Right part: magnification x5000. A, emerged area; B, intermittently immersed area; C, immersed area. The white arrows indicate the flow direction.

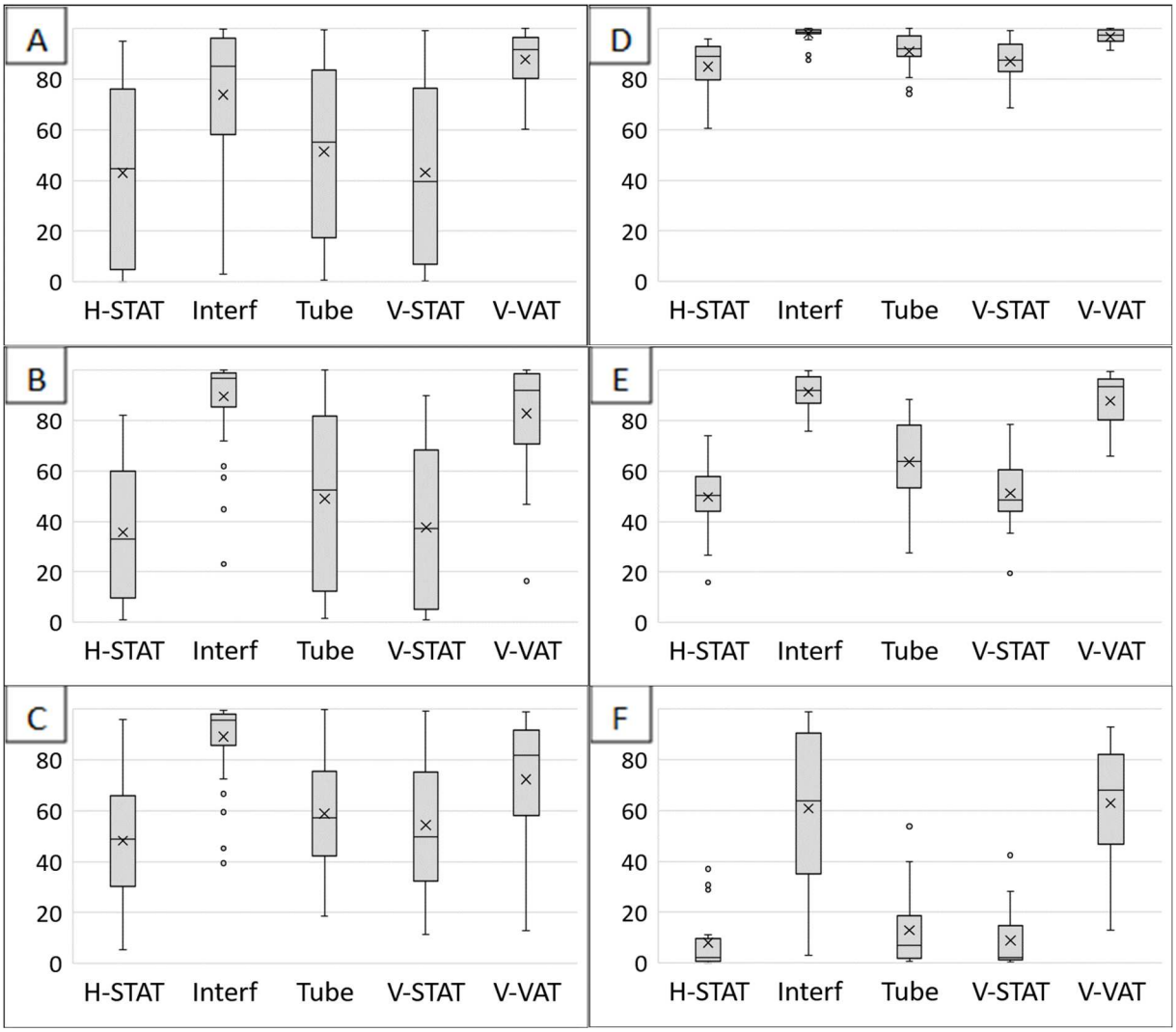

Figure 4: Residual ratio (x100) of biofilms after mechanical detachment versus areas. A, B, C: shear stress values were not taken into account (A: 24 h-biofilm; B: 48 h-biofilm; C: 72 h-biofilm); D, E, F: times of biofilm formation were not taken into account (C: 17 Pa, D: 130 Pa, E: 360 Pa).

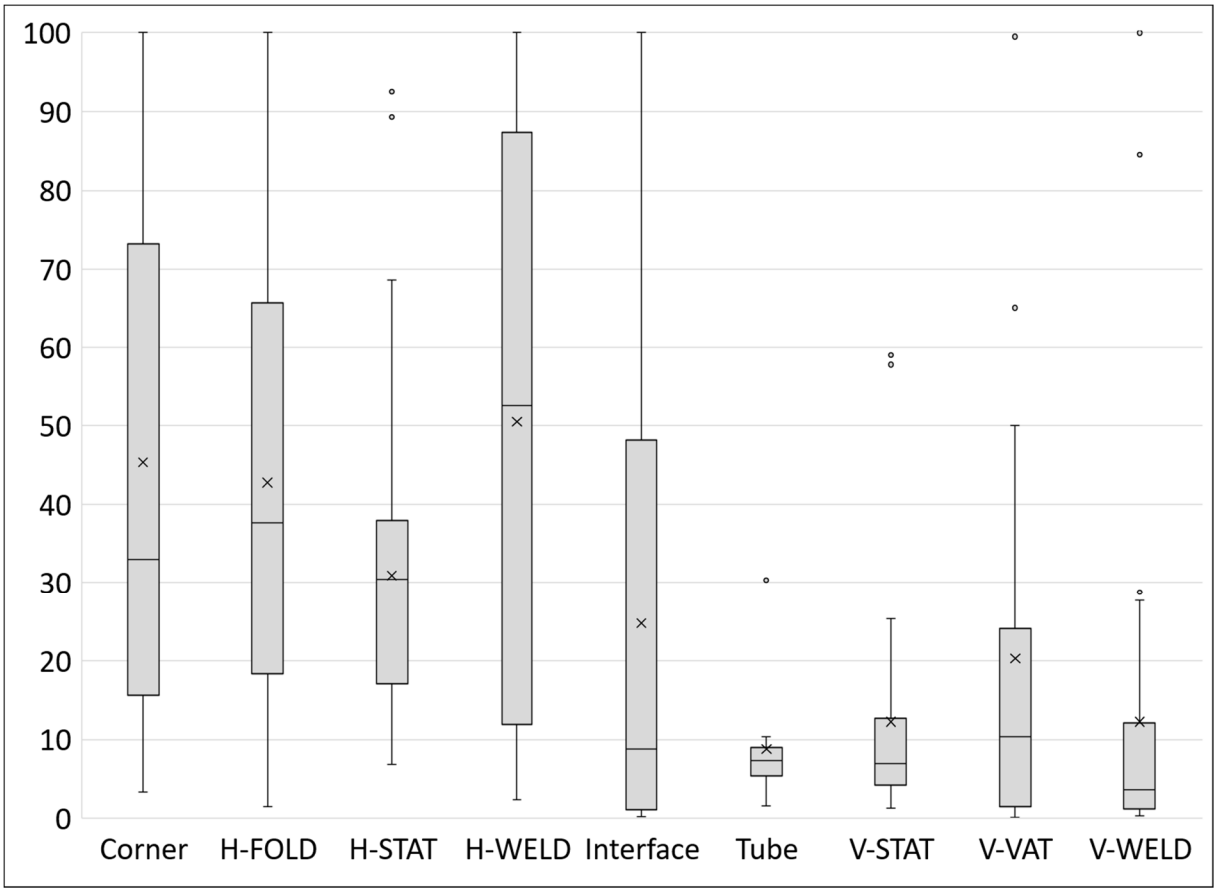

Figure 5: Box plots of the residual ratio (x100) of biofilms after cleaning by enzymes versus areas, all the data were taken into account whatever the biofilm age.

Device	Location/ Geometry	Flow condition and average wall shear stress [WSS] ($\bar{\tau}_w$)	Sample name	Biofilm Formation: Enumeration	Biofilm Formation: SEM	Biofilm Removal: Foam cleaning	Biofilm Removal: Mechanical detachment
Tubes	Bottom/Flat	1-D flow $\bar{\tau}_w$ = 0.45 Pa	Square tubes	X	X	X	X
Entry vat	Bottom/Flat	Static $\bar{\tau}_w$ < 0.01 Pa	H-Static	X	X	X	X
	Side/Flat	Static $\bar{\tau}_w$ < 0.01 Pa	V-Static	X	X	X	X
Test vats	Bottom/Flat	3D flow / 0.5 < $\bar{\tau}_w$ < 4 Pa	H-Vat	X	X *	X	
	Side/Flat	3D flow / 0.5 < $\bar{\tau}_w$ < 4 Pa	V-Vat	X	X	X	X
	Side/Flat	Air/Liquid/Wall Interface	Interface	X	X	X	X
	Bottom/Weld	3D flow / 0.1 < $\bar{\tau}_w$ < 5 Pa	H-Weld	X	X	X	
	Side/Weld	3D flow / 0.1 < $\bar{\tau}_w$ < 5 Pa	V-Weld	X		X	
	Bottom/Fold	3D flow / 0.1 < $\bar{\tau}_w$ < 5 Pa	H-Fold	X	X	X	
	Bottom-Side/ Fold & Weld	3D flow / $\bar{\tau}_w$ = 0.1 Pa	Corner	X		X	

** Biofilms analysed on the bottom side of the right-angled coupons*

Table 1: Description of the locations where coupons were installed and list of the analyses implemented

Areas	Biofilm 24 h							Biofilm 48 h								Biofilm 72 h						
	Mean	Tukey's grouping[a]						Mean	Tukey's grouping[a]							Mean	Tukey's grouping[a]					
H-static	6.116	A						7.892	A							8.279	A					
Square Tubes	5.300		B					7.326	A	B	C					8.161	A					
V-Static	5.925	A	B					7.551	A	B						8.036	A	B				
Corner	5.656	A	B					6.912		B	C					7.397		B	C			
Interface	3.567			C	D			6.026				D	E			7.359			C			
H-Vat	3.080				D			5.539					E	F		7.134			C			
V-Weld	3.872			C				5.051						F		7.031			C			
H-Weld	5.226		B					6.576			C	D				6.833			C	D		
H-Fold	3.392			C	D			5.750					E	F		6.349				D		
V-Vat	0.849						E	3.507							G	5.492						E

[a] Following Tukey's grouping, areas with no common letter are significantly different.

Table 2: Amounts of biofilms produced in the different locations and grouping of biofilms, according to the Tukey's grouping (p-value < 0.05)

	Model		Parameters taken into account		
Model	**Pr > F**	**R^2**	**Pr > F Location**	**Pr > F Trial**	**Pr > F Age**
Biofilm 24, 48 & 72 h	<.0001	0.7603	<.0001	0.0006	<.0001
Biofilm 24 h	<.0001	0.8327	<.0001	0.8947	-
Biofilm 48 h	<.0001	0.7389	<.0001	0.0188	-
Biofilm 72 h	<.0001	0.4904	<.0001	0.0001	-

-: not applicable

Table 3. Information obtained from the analysis of variance achieve to investigate the role of Coupon location, trial and biofilm age on the amount of biofilm. A further grouping of biofilms was performed according to the Tukey's grouping (p-value < 0.05)

	Model		Parameters taken into account			
Model	**Pr > F**	**R^2**	**Pr > F Location**	**Pr > F Trial**	**Pr > F Time**	**Pr > F WSS**
Mechanical detachment (biofilm 24, 48 & 72 h)						
All WSS	<.0001	0.7535	<.0001	0.0005	0.1162	<.0001
WSS 17 Pa	<.0001	0.5450	<.0001	0.0040	0.0580	-
WSS 60 Pa	<.0001	0.7077	<.0001	0.0029	0.1481	-
WSS 130 Pa	<.0001	0.7433	<.0001	0.0388	0.5130	-
WSS 190 Pa	<.0001	0.7682	<.0001	0.0752	0.5777	-
WSS 275 Pa	<.0001	0.7414	<.0001	0.8857	0.0302	-
WSS 360 Pa	<.0001	0.6637	<.0001	0.9987	0.0202	-
Enzymatic cleaning (biofilm 24, 48 & 72 h)						
WSS 0 Pa	<.0001	0.2569	<.0001	0.0122	0.9100	-

-: not applicable

Table 4. Influence of the sample, trial, time of biofilm formation and shear stress on the ratio of residual biofilm. Two analyses of variance were performed for the mechanical detachment. The first analysis took into account the whole set of data (17, 60, 130, 190, 275, and 360 Pa). In the second analysis, each wall shear stress was analysed separately. The third analysis concerns enzymatic cleaning data.

Table 5.1	Tukey's grouping[a]				
WSS	Interface	V-VAT	Tube	V-STAT	H-STAT
17 Pa	A	A	B	BC	C
60 Pa	A	A	B	C	C
130 Pa	A	B	B	C	C
190 Pa	A	A	B	BC	C
275 Pa	A	A	B	B	B
360 Pa	A	A	B	B	B

Table 5.2		Tukey's grouping[a]						
H-WELD	**Corner**	**H-FOLD**	**H-STAT**	**Interface**	**V-VAT**	**V-WELD**	**V-STAT**	**Tube**
A	AB	AB	AB	ABC	BC	C	C	C

[a]*Following Tukey's grouping, areas with no common letter are significantly different in terms of ease of removal; group A is the most resistant to detachment whereas group C is the least resistant.*

Table 5: Tukey's grouping of biofilms according to their resistance to mechanical detachment (Table 5.1) and enzyme cleaning including bend surfaces (Table 5.2) (p-value < 0.05)